

Di-Boson Physics at the Tevatron

A. T. Goshaw (for the CDF and DØ Collaborations)

Duke University, Durham, NC 27708

Received: date / Revised version: date

Abstract. A summary is presented of recent measurements of di-boson production at the Tevatron. The results from the CDF and DØ experiments are based upon 130-320 pb^{-1} of $p\bar{p}$ collisions at $\sqrt{s} = 1.96$ TeV. The $W\gamma$, $Z\gamma$, WW , and WZ production properties are compared to Standard Model predictions, and limits extracted for anomalous triple gauge couplings.

PACS. PACS-key describing text of that key – PACS-key describing text of that key

1 Introduction

A study of di-boson production at the Tevatron provides a rich source of electroweak Standard Model (SM) tests, is sensitive to new physics signatures, and opens a window into the challenges faced in searches for the Higgs boson. In this report we summarize measurements made by the CDF and DØ collaborations based upon the first significant data sets obtained from Run II of the Tevatron. The production channels are $p\bar{p} \rightarrow VV' + X$ at $\sqrt{s} = 1.96$ TeV, where the di-boson pairs are $W\gamma$, $Z\gamma$, WW , and WZ . Figure 1 shows the expected cross sections based upon SM predictions. The di-boson cross sections of interest in this review range from about 1 to 10 pb.

For these di-boson production channels, the measured cross sections and kinematic distributions are compared to leading order electroweak predictions, scaled to correct for lowest order QCD effects. Anomalous coupling parameters describing the triple gauge vertices are used as a metric for evaluating the sensitivity to new physics. This assumes that these will appear as deviations of the W and Z bosons from point particles. There are of course other sources of new physics that would appear in di-boson production, perhaps the most likely source of discoveries at the Tevatron.

Di-boson studies at the Tevatron compliment those made at LEP in several ways. Some of the triple gauge couplings (TGC's) can be better isolated using $q\bar{q}'$ collisions. For example $q\bar{q}' \rightarrow W^* \rightarrow W\gamma$ depends only on the $WW\gamma$ coupling, while $q\bar{q}' \rightarrow W^* \rightarrow WZ$ depends only on the WWZ coupling. In addition the higher parton collision energy at the Tevatron explores different dynamic regions of the TGC, and opens up the possibility for the direct production of massive particles decaying into final states with di-bosons. Measurements of W/Z hadronic decay channels paired with a photon or a W/Z leptonic decay are useful for studies of dijet mass resolution, and provide

calibration channels for searches for the Higgs boson in W/Z $H(b\bar{b})$.

2 W boson production with a photon

The reaction $p\bar{p} \rightarrow l\nu\gamma$ has contributions from W bosons produced with initial and final state photon radiation and from the direct $WW\gamma$ coupling. A study of $l\nu\gamma$ events allows extraction of the $WW\gamma$ coupling parameters, assuming that the W and photon couplings to fermions are described by the SM. Under the assumption of Lorentz and electromagnetic gauge invariance, and neglecting CP violating terms, the effective Lagrangian is [1]:

$$L_{WW\gamma} = -ie[(W_{\mu\nu}^\dagger W^\mu A^\nu - W_\mu^\dagger A_\nu W^{\mu\nu}) + \kappa_\gamma W_\mu^\dagger W_\nu F^{\mu\nu} + \lambda_\gamma/M_W^2 W_{\lambda\gamma}^\dagger W_\nu^\mu F^{\nu\lambda}].$$

In the SM at tree level $\Delta\kappa_\gamma = \kappa_\gamma - 1 = 0$ and $\lambda_\gamma = 0$. Deviations of the coupling parameters from the SM values are usually parameterized with a dipole form factor to preserve tree-level unitarity at high energies: $\Delta\kappa_\gamma = \Delta\kappa_{o\gamma}/(1+s/\Lambda^2)^2$ and $\lambda_\gamma = \lambda_{o\gamma}/(1+s/\Lambda^2)^2$ where \sqrt{s} is the $W\gamma$ invariant mass and Λ sets the energy scale of new physics.

The results presented here use W decays to electrons ($E_t > 25$ GeV) and muons ($P_T > 20$ GeV/c) in association with central photons ($|\eta| < 1.0$). To suppress final state bremsstrahlung, the photon is isolated from the lepton by $\Delta R(l-\gamma) > 0.7$. The number of event candidates is 323 (273) in the CDF (DØ) experiments using integrated luminosity of 130-200 pb^{-1} . The background is dominated by W+jet events in which the jet passes the photon selection cuts. The resulting signal/background ratios vary from 0.8 to 1.9 depending on channel and experiment. For details see references [2] and [3].

Table I shows cross sections for $p\bar{p} \rightarrow l\nu\gamma$. These are an average of the measurements from the electron and muon decay channels, and corrected for the full W boson decay phase space. The photons have $\Delta R(l-\gamma) > 0.7$, and

Table 1. Cross Sections for $p\bar{p} \rightarrow l\nu\gamma$ with $\Delta R(l-\gamma) > 0.7$

	$E_T(\gamma)$	$\sigma_{data}(l\nu\gamma)$ pb	$\sigma_{SM}(l\nu\gamma)$ pb
CDF	> 7 GeV	18.1 ± 3.1	19.3 ± 1.4
DØ	> 8 GeV	14.8 ± 2.1	16.0 ± 0.4

$E_T(\gamma)$ above the cuts indicated in the table. The photon E_T distribution from the CDF-selected $l\nu\gamma$ events is shown in Figure 2. The transverse mass spectrum of the $W\gamma$ system from DØ data is presented in Figure 3. The upper histograms are the SM predictions for $p\bar{p} \rightarrow l\nu\gamma$ plus backgrounds. All the data are consistent with SM predictions.

Anomalous $WW\gamma$ couplings would enhance the production of high E_T photons. The DØ Collaboration [3] has used their data to put limits on $\Delta\kappa_{o\gamma}$ and $\lambda_{o\gamma}$ using a dipole form factor with $\Lambda = 2$ TeV. Holding one parameter at the SM value of zero and allowing the other to vary, the 95% CL's are: $-0.88 < \Delta\kappa_{o\gamma} < 0.96$ and $-0.20 < \lambda_{o\gamma} < 0.20$.

3 W^+W^- and $W^\pm Z$ boson pair production

The production of $W^\pm Z$ pairs depends on the WWZ trilinear coupling, while W^+W^- production is sensitive to both $WW\gamma$ and WWZ couplings. In Section 1 the anomalous coupling parameters for the $WW\gamma$ vertex were introduced: $\Delta\kappa_{o\gamma}$ and $\lambda_{o\gamma}$. Under the same assumptions the WWZ vertex is described by the Lagrangian [4]:

$$L_{WWZ} = -ie\cot(\theta_W)g_1^Z[(W_{\mu\nu}^\dagger W^\mu A^\nu - W_\mu^\dagger A_\nu W^{\mu\nu}) + \kappa_Z W_\mu^\dagger W_\nu F^{\mu\nu} + \lambda_Z/M_W^2 W_{\lambda\gamma}^\dagger W_\nu^\mu F^{\nu\lambda}]$$

In the SM $\Delta g_1^Z = g_1^Z - 1 = 0$, $\Delta\kappa_Z = \kappa_Z - 1 = 0$ and $\lambda_Z = 0$. As discussed previously, deviations from these SM values need to be suppressed by a form factor, usually taken of the form $\lambda_Z = \lambda_{oZ}/(1+s/\Lambda^2)^2$, etc. Therefore a description of the $WW\gamma$ and WWZ vertices requires five parameters: $\Delta\kappa_{o\gamma}$, $\lambda_{o\gamma}$, Δg_{o1}^Z , $\Delta\kappa_{oZ}$, and λ_{oZ} plus the scale of the new physics set by Λ .

3.1 W^+W^- measurements

The SM cross section for $p\bar{p} \rightarrow W^+W^- + X$ at $\sqrt{s} = 1.96$ TeV is 12.4 ± 0.8 pb [5]. The CDF [6] and DØ [7] collaborations have made measurements using the leptonic W^+W^- decay channels $l\nu l'\nu$ with $l, l' = e$ or μ . The branching ratio is only 4.6 % but the data have low backgrounds. The number of W^+W^- candidates is 25 (17) for DØ (CDF) using about 200 pb^{-1} of data. After all selection cuts both experiments attained a signal over background of about 2.2. Correcting for decay branching ratios, the W^+W^- pair inclusive cross sections are measured to be:

$$\begin{aligned} &13.8_{-3.8}^{+4.8}(\text{stat.})_{-0.9}^{+1.2}(\text{sys.}) \pm 0.9(\text{lum.}) \text{ pb (DØ)} \\ &14.6_{-5.1}^{+5.8}(\text{stat.})_{-3.0}^{+1.8}(\text{sys.}) \pm 0.9(\text{lum.}) \text{ pb (CDF)}. \end{aligned}$$

These total W^+W^- cross sections are plotted in Figure 4, compared to the SM prediction. The lepton P_T spectrum from the W^+W^- decays is presented in Figure 5. All the data are in good agreement with SM expectations.

The CDF collaboration has also studied the W^+W^- channel using $W \rightarrow l\nu$ events with at least two jets having $32 < M_{jj} < 184$ GeV/ c^2 . The analysis searches for a $W \rightarrow$ jet-jet mass peak (broadened by a small $Z \rightarrow$ jet-jet contribution) above the large di-jet QCD background. No signal is seen in 200 pb^{-1} of data. A 95% CL limit is put on the $W^+W^- + W^\pm Z$ cross section of 46 pb, compared to the SM prediction of 16 ± 1 pb. Anomalous couplings would cause an excess of events with high $W P_T$. Using a di-jet signal region $56 < M_{jj} < 112$ GeV/ c^2 , the lack of an excess of $W(l\nu)$ bosons at high P_T can be used to put limits on the $WW\gamma$ and WWZ anomalous coupling parameters. The analysis assumes that $\Delta g_{o1}^Z = 0$, $\Delta\kappa_o = \Delta\kappa_{oZ} = \Delta\kappa_{o\gamma}$ and $\lambda_o = \lambda_{oZ} = \lambda_{o\gamma}$. Setting one of the parameters zero, the limits on the anomalous couplings are: $-0.48 < \Delta\kappa_o < 0.56$ and $-0.41 < \lambda_o < 0.39$, using a dipole form factor with $\Lambda = 1$ TeV.

3.2 $W^\pm Z$ measurements

The SM cross section for $p\bar{p} \rightarrow W^\pm Z + X$ at $\sqrt{s} = 1.96$ TeV is 3.7 ± 0.3 pb [5]. The DØ collaboration [8] has searched for $W^\pm Z$ events in the decay channels $l'\nu l^+l^-$ using electrons and muons. With 300 pb^{-1} of data, after all selection cuts, two 3- μ and one 3- e events are isolated with a total background of 0.71 ± 0.08 events. The 95 % CL on the production cross section is 13.3 pb, consistent with the SM expectations. By setting two of the three anomalous coupling parameters at their SM value of zero, 95 % CL can be set on the third. Using a scale $\Lambda = 1.5$ TeV, the results are: $-0.48 < \Delta\kappa_{oZ} < 0.48$ and $-0.49 < \Delta g_{o1}^Z < 0.66$ with no limits on $\Delta\kappa_{oZ}$.

4 Z boson production with a photon

The SM predictions for the reaction $p\bar{p} \rightarrow l^+l^-\gamma$ include Z/γ^* production with bremsstrahlung from the initial state quarks or final state radiation from the decay l^+l^- pairs. Since the SM couplings $ZZ\gamma$ and $Z\gamma\gamma$ are zero, new physics effects would appear as deviations from bremsstrahlung predictions. Under the assumption of Lorentz and electromagnetic gauge invariance, the most general Lagrangian [10] includes 8 complex parameters of the form $h_i^V = h_{oi}^V/(1+s/\Lambda^2)^n$ where $V = Z$ or γ and $i = 1-4$. Again multipole form factors are needed to preserve unitarity at high energy.

As for the $W\gamma$ measurements, the events are triggered on high E_T central electrons or muons, and events selected with charged lepton pairs and an isolated photon with $\Delta R(l-\gamma) > 0.7$. The number of event candidates are 290 (70) for the DØ (CDF) experiments using 200-320 pb^{-1} of data. Backgrounds are low dominated entirely by Z +jet events with the jet passing the photon selection cuts. Depending

Table 2. Cross Sections for $p\bar{p} \rightarrow l^+l^-\gamma$ with $\Delta R(l-\gamma) > 0.7$

	$E_T(\gamma)$	$M(l_+l_-)$	σ_{data} pb	σ_{SM} pb
CDF	> 7 GeV	> 40 GeV/ c^2	4.6 ± 0.6	4.5 ± 0.3
DØ	> 8 GeV	> 30 GeV/ c^2	4.2 ± 0.5	3.9 ± 0.2

on channel and experiment the signal/background varies from 6 to 15. For details see references [2] and [9].

Table 2 shows cross sections for $p\bar{p} \rightarrow l^+l^-\gamma$, from averages of the electron and muon decay channels and corrected for the Z/γ^* decay phase space. The photons have $\Delta R(l-\gamma) > 0.7$ and have the minimum $E_T(\gamma)$ and $M(l_+l_-)$ shown in the table. Figure 6 shows the photon E_T spectrum from the CDF data, and Figure 7 the invariant mass $M(l\bar{l}\gamma)$ from DØ measurements. The lower solid histograms are the backgrounds from $Z + \text{jet}$ events with the jet passing photon selection cuts. The upper histograms are the sum of the background plus electroweak predictions for $p\bar{p} \rightarrow l^+l^-\gamma$ production. Both the measured total cross sections and the kinematic distributions are in good agreement with the SM.

The DØ Collaboration [9] has used their data to put limits on the anomalous coupling parameters h_{oi}^Z and h_{oi}^γ using $\Lambda = 1$ TeV. As for the other limits, all parameters but one are set at their SM values and 95% CL are determined for the remaining parameters: $|h_{10,30}^Z| < 0.23$; $|h_{20,40}^Z| < 0.020$; $|h_{10,30}^\gamma| < 0.23$; $|h_{20,40}^\gamma| < 0.019$.

5 Summary and Conclusions

Using 130-320 pb^{-1} of $p\bar{p}$ collisions at $\sqrt{s} = 1.96$ TeV, the CDF and DØ Collaborations have measured di-boson production and compared the data to SM predictions. Deviations of the measured cross section from nominal NLO SM predictions are summarized in Table 3, where the uncertainties quoted are the quadrature sum of the experimental statistical and systematic errors. All results are in good agreement with the SM.

Measurements of the P_T spectra of the bosons can be used as a more sensitive probe for new physics. Substructure of the W or Z, or massive particles decaying to di-bosons, would cause an excess of high P_T bosons. No excesses are observed in the photon, W or Z spectra. One way to quantify this is in terms of limits on anomalous TGC parameters. These are summarized in Table 4.

The diboson data described in this report represents 3-6 % of that expected from the Tevatron. Further increases in sensitivity will be attained by combing the CDF and DØ data, and doing joint analyses combining di-boson channels. In addition to the potential for discoveries in this data, the techniques developed will enhance the potential for Higgs boson discoveries at the Tevatron and LHC.

6 Acknowledgements

I would like to thank my CDF colleagues and members of the DØ collaboration, particularly Tom Diehl and Andrew

Table 3. Cross section comparisons to Standard Model predictions

Channel ($l=e$ or μ)	$(\sigma_{data} - \sigma_{SM}) / \sigma_{SM}$
$W\gamma$ [$l\nu\gamma$]	-0.06 ± 0.16 CDF -0.06 ± 0.16 DØ
$Z\gamma$ [$ll\gamma$]	$+0.02 \pm 0.13$ CDF $+0.08 \pm 0.13$ DØ
WW [$llll$]	$+0.17 \pm 0.42$ CDF $+0.10 \pm 0.32$ DØ
Cross section limits	σ_{data} (95% C.L.)/ σ_{SM}
WZ [$l\nu ll$]	3.3 DØ
$WZ + WW$ [$l\nu qq$]	2.4 CDF
$WZ + ZZ$ [$ll(l\nu$ or $\nu\nu)$]	3.0 CDF

Table 4. Triple gauge boson anomalous coupling limits

Coupling	limits at 95% C.L.	Energy scale Λ
$WW\gamma$	$-0.88 < \Delta\kappa_{o\gamma} < 0.96$ $-0.20 < \lambda_{o\gamma} < 0.20$	2 TeV
WWZ	$-0.49 < \Delta g_1^Z < 0.66$ $-0.48 < \Delta\kappa_{oZ} < 0.48$	1.5 TeV
$ZZ\gamma$	$ h_{10,30}^\gamma < 0.23$ $ h_{20,40}^\gamma < 0.019$	1 TeV
ZZZ	$ h_{10,30}^Z < 0.23$ $ h_{20,40}^Z < 0.020$	1 TeV
WWZ and $WW\gamma$	$-0.48 < \Delta\kappa_o < 0.56$ $-0.41 < \lambda_o < 0.39$	1.5 TeV

Askew, for access to the data presented in this report. It was a pleasure to participate in the HCP05 conference, and have the opportunity to present this overview. I thank the organizing committee for giving me this opportunity.

References

- U. Baur and E. Berger, Phys. Rev. D **41**, 1476 (1990).
- D. Acosta *et al.*, The CDF Collaboration, Phys. Rev. Lett. **94**, 040803 (2005).
- V. Abazov *et al.*, The DØ Collaboration, Phys. Rev. D **71**, 091108 (2005).
- Haigawara, Peccii and Zeppenfeld, Nuc. Phys. B **282**, 253 (1987).
- J. M. Campbell and R.K. Ellis, Phys. Rev. D **62**, 114012 (2000).
- D. Acosta *et al.*, The CDF Collaboration, Phys. Rev. Lett. **94**, 211801 (2005).
- V. Abazov *et al.*, The DØ Collaboration, Phys. Rev. D **94**, 151801 (2005).
- V. Abazov *et al.*, The DØ Collaboration, hep-ex/0504019 (2005).
- V. Abazov *et al.*, The DØ Collaboration, Phys. Rev. Lett. **95**, 051802 (2005).
- J. Ellison and J. Wudka, Ann. Rev. Nucl. Part. Sci. **48**, 33-80 (1998).

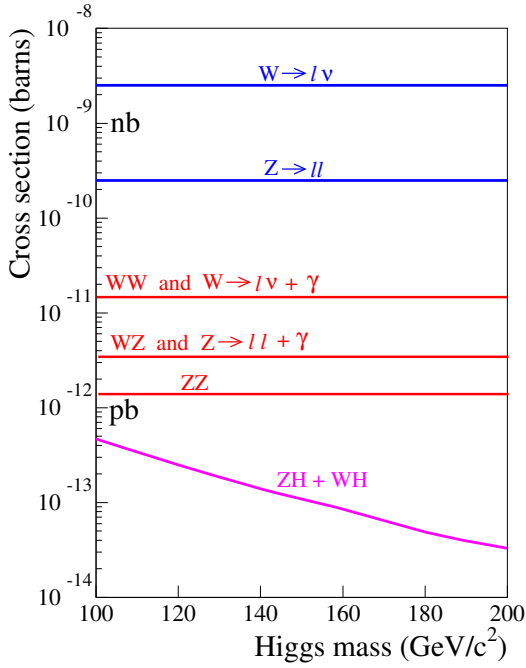


Fig. 1. Standard model predictions for boson and di-boson production cross sections.

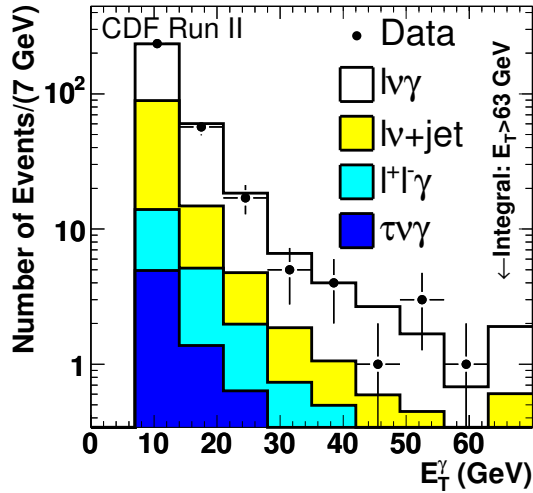


Fig. 2. Photon P_T spectrum from $p\bar{p} \rightarrow l\nu\gamma$ events.

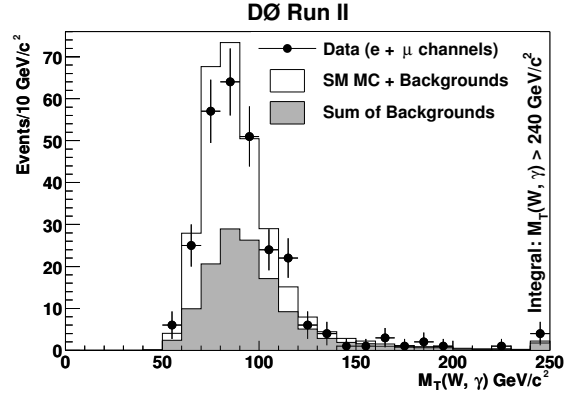


Fig. 3. Transverse mass of $W\gamma$ system from $p\bar{p} \rightarrow l\nu\gamma$ events.

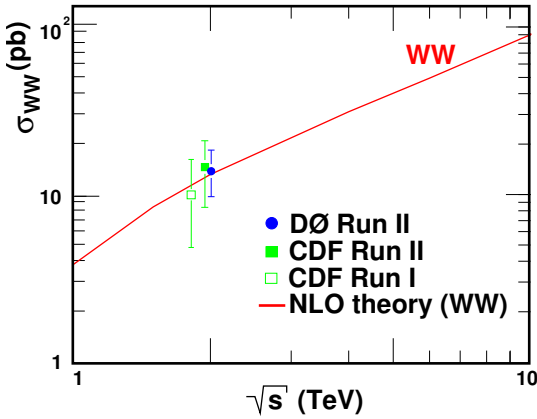


Fig. 4. Measured $p\bar{p} \rightarrow W^+W^-$ inclusive cross sections compared to the NLO SM prediction.

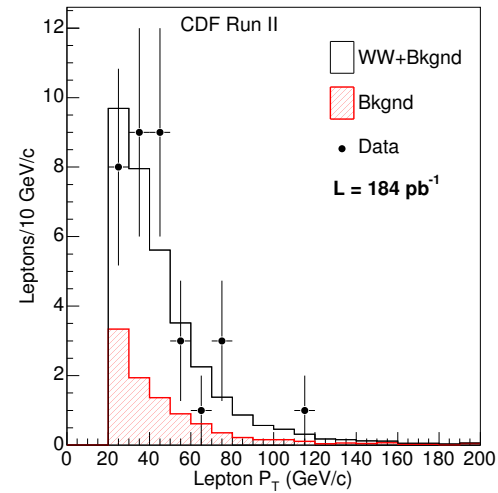


Fig. 5. Lepton P_T spectrum from $p\bar{p} \rightarrow W^+W^-$ events.

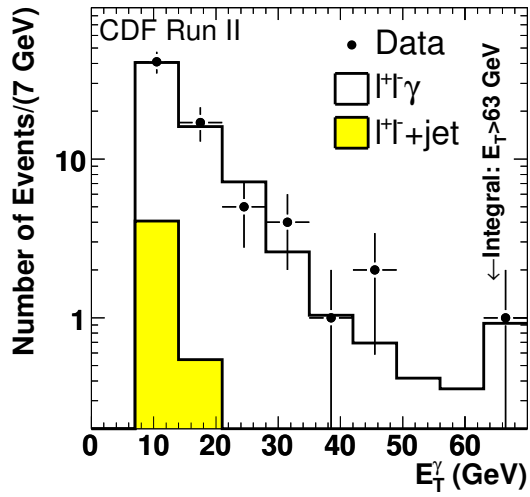


Fig. 6. Photon P_T spectrum from $p\bar{p} \rightarrow ll\gamma$ events.

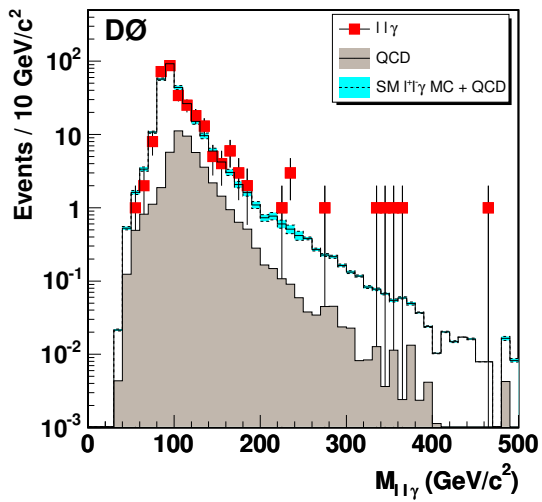


Fig. 7. Mass of $ll\gamma$ system from $p\bar{p} \rightarrow ll\gamma$ events.